Tokamak Two-Fluid Ignition Conditions

L. Guazzotto[1,*] and R. Betti [2]

[1]Physics Department, Auburn University, Auburn, AL, 36849
[2]Department of Mechanical Engineering, University of Rochester, Rochester, NY, 14627

July 7, 2017

Abstract

This work focuses on modeling the properties needed by a plasma to reach ignition, where ignition is the condition in which fusion power is produced at steady state without any external input power. We extend the classic work by Lawson giving the $p_{tot}\tau_E$ (product between density, temperature and energy confinement time) needed for ignition [J. D. Lawson, Proc. Phys. Soc. London **Sect. B 70**, 6 (1957)] by improving the original zero-dimensional, single fluid model. The effect of multi-fluid physics is included, by distinguishing ions, electrons and α particles. The effects of one-dimensional density and temperature profiles are also considered. It is found that the multi-fluid model predicts a larger Lawson product required for ignition than the single-fluid one. A detailed analysis of the energy confinement times for each species and energy equilibration times between species shows that the electron energy confinement time is the parameter more strongly affecting the Lawson product needed for ignition. It is also found that peaked profiles (of either temperature or density) require a smaller Lawson product for ignition than flat profiles.

I Introduction

Modern experiments based on the magnetic confinement approach for nuclear fusion have been edging close to the breakeven point, where the power

*Author to whom correspondence should be addressed. Email: luca.guazzotto@auburn.edu

produced by nuclear fusion reactions exceeds the power needed to heat and confine the plasma. [1] The generation of experiments currently under construction, with particular reference to ITER [2] is designed to explore the "burning plasma" state, with a α-heating power produced by fusion reactions larger than the input power for long durations during plasma discharges of duration much longer than any characteristic plasma time scale. This is customarily indicated using the gain factor Q, defined as the ratio between net output power and input power, with values of $Q > 1$ corresponding to burning plasmas. The next future step in plasma performance is the achievement of a value of "$Q = \infty$", corresponding to energy production without any input power. This situation is commonly known as "ignition" and is the ultimate goal of magnetic fusion research. A general discussion of ignition and burning plasma issues can be found e.g. in Refs. [3, 4] and references within.

The question of how to characterize the plasma properties needed to achieve ignition has been of interest since the beginning of the nuclear fusion enterprise. The classical work by Lawson [5] showed that a certain minimum triple product $nT\tau_E$ must be exceeded in order to reach ignition, where n is the plasma density, T the plasma temperature and τ_E the energy confinement time. Lawson's triple product required for ignition is a function of plasma temperature and has a minimum for $T \simeq 14$ [keV]. The work in Ref. [5] has been referenced for decades as the standard figure of merit for plasma performance and does indeed highlight some fundamental plasma properties that experiments need to aim for. Even so, the model in Ref. [5] is extremely and unrealistically simplified. In particular, both density and temperature profiles are assumed to be constant across the plasma cross section ("0D model") and a single-fluid approach is used, in which no distinction is made between ion and electron properties and the power produced by fusion reactions is delivered to the plasma immediately and without losses. Perhaps surprisingly, no significant or at least no widely recognized improvements to the model have been made since the original work was first published. [6–9]

Several improvements to Lawson's criterion are considered in this work. More in detail, we consider two different ways to obtain a more realistic picture of fusion-relevant plasmas. First, we treat ions, electrons and alpha particles as different fluids, which exchange energy through physical processes (equilibration and slowing down times). Moreover, each species can lose energy to the external environment independently, i.e. at different rates. Second, we allow density and temperatures to have non-constant profiles in the plasma cross section. As a natural extension of Lawson's 0D approach,

one-dimensional profiles are considered in this work. Even though this is still not an extremely accurate depiction of experimental properties, in particular for strongly-shaped and three-dimensional plasmas, it is certainly a step forward from existing models. Some of the effect of multi-fluid and one-dimensional physics have been considered in Refs. [10, 11]. Recognizing that a great merit of the Lawson criterion is in its simplicity, we provide analytical expressions that approximate the numerical results obtained with the more detailed description of the plasma. In particular (see Section II), it is shown that the modified 0D Lawson criterion is well approximated by the formula

$$p_{tot}\tau_{Ei} \simeq a_0 \left(1+\frac{a_1}{c_2}\right)\left(1+\frac{a_2}{c_4}\right)+\frac{a_3}{c_2 c_4}+a_4\log(c_4), \tag{1}$$

where $c_2 \equiv \tau_{Ee}/\tau_{Ei}$, $c_4 \equiv \tau_{E\alpha}/\tau_{Ei}$ (τ_{Ej} is the energy confinement time of each species, ion, electrons and αs) and all a_j coefficients are listed in Table 1.

The remainder of this paper is organized as follows. In Section II the effects of multi-fluid physics are analyzed still in the (0D) limit of constant profiles. Section III describes the effect of one-dimensional density and temperature variations in the plasma profiles. Concluding remarks are contained in Section IV.

II Multi-Fluid Physics in 0-D

We start our investigation by adopting a model similar to the classic Lawson one, but considering in more detail the distinct properties of ion, electrons. In this section and in the remainder of the paper a notation similar to the notation in Ref. [1] will be used. Ions and electrons are described as separate fluids. Under the assumption of quasi-neutrality, they share the same number density n, but are allowed to have different (in general, time-dependent) temperatures T_i and T_e. As for α particles, they are described as a separate fluid, with number density n_α. In time-dependent form, these assumptions lead to the energy-balance equations:

$$\frac{3}{2}n\frac{\partial T_i}{\partial t} = S_{hi} - \frac{3}{2}\frac{p_i}{\tau_{Ei}} + \frac{3}{2}\frac{n(T_e-T_i)}{\tau_{eq}} \tag{2}$$

$$\frac{3}{2}n\frac{\partial T_e}{\partial t} = S_{he} - \frac{3}{2}\frac{p_e}{\tau_{Ee}} + \frac{n_\alpha}{\tau_\alpha}E_\alpha - C_B\frac{p_e^2}{T_e^{3/2}} + \frac{3}{2}\frac{n(T_i-T_e)}{\tau_{eq}} \tag{3}$$

$$\frac{\partial n_\alpha}{\partial t} = \frac{n^2}{4}<\sigma v> - \frac{n_\alpha}{\tau_\alpha} - \frac{n_\alpha}{\tau_{E\alpha}}. \tag{4}$$

This compares to the single-fluid energy balance [1]

$$\frac{3}{2}n\frac{\partial T}{\partial t} = \frac{E_\alpha}{16}p^2\frac{<\sigma v>}{T^2} + S_h - \frac{C_B}{4}\frac{p^2}{T^{3/2}} - \frac{3}{2}\frac{p}{\tau_E}. \tag{5}$$

Equations (2-4) contain all the information used in the 0-D model. The terms S_{hi} and S_{he} are the ion and electron external heating powers (the latter will be assumed to be 0 in the rest of this work). For each fluid, thermal energy losses are expressed by the ratio between the internal energy (proportional to the pressure $p_j = nT_j$) and a characteristic energy confinement time τ_{Ej}. For simplicity, α particles are assumed to be locally deposited with the time scale of the α slowing down time τ_α so α losses to the outside of the plasma are expressed in terms of number density losses. Two coupling times are included in the model, the α slowing-down time τ_α (time to couple α energy to the electrons, observe that no α power is directly coupled to the ions) and the ion-electron temperature equilibration time τ_{eq}. Finally, C_B is the coefficient for Bremsstrahlung emission (which only depends on electron temperature) and E_α is the α particle energy. We will only consider a deuterium-tritium plasma in the present work. Except where otherwise specified, the physical equilibration times [1, 12] are used:

$$\tau_{eq} = \frac{1}{78\times 10^{-20}n}\left(\frac{T_e+T_i}{2}\right)^{3/2}, \tag{6}$$

$$\tau_\alpha = 1.17\times 10^{18}\frac{T_e^{3/2}}{n}, \tag{7}$$

where densities are in m^{-3}, temperatures in keV and times are in seconds. Both equilibration times are strong functions of temperature monotonically increasing with temperature. For reference, both are $\simeq 1$ second for $n \simeq 10^{20}\mathrm{m}^{-3}$ and $T_i \simeq T_e \simeq 20$keV.

In order to make meaningful comparisons with the single-fluid results, an average energy confinement time

$$\hat{\tau}_E \equiv 2\frac{\tau_{Ei}\tau_{Ee}}{\tau_{Ei}+\tau_{Ee}} \tag{8}$$

is defined. Results will be expressed in terms of $\hat{\tau}_E$ and/or τ_{Ei} in the following. The ion confinement time τ_{Ei} is used because more accurate predictions for its value are available than for the electron energy confinement time τ_{Ee}. [3]

The first task is to derive a multi-fluid version of the Lawson criterion. That is accomplished by setting time derivatives to 0 in Eqs. (2-4). Writing

$$\tau_{Ei} \equiv k_i \hat{\tau}_E, \tag{9}$$

$$\tau_{Ee} \equiv k_e \hat{\tau}_E \tag{10}$$

for convenience (note that if $\hat{\tau}_E$ is assigned from input, *one* of k_i and k_e must also be assigned), the energy balance equation for ignition reduces to

$$\frac{n}{4} < \sigma v > \frac{\tau_{E\alpha}}{\tau_{E\alpha} + \tau_\alpha} E_\alpha - C_B n \sqrt{\frac{k_i \hat{\tau}_E + \tau_{eq}}{k_i \hat{\tau}_E} T_i} - \frac{3}{2} \left(\frac{2}{\hat{\tau}_E} + \frac{\tau_{eq}}{k_i k_e \hat{\tau}_E^2} \right) T_i \geq 0. \tag{11}$$

Even though Eq. (11) can be solved analytically for $\hat{\tau}_E$, the solution is very cumbersome and not very informative. A more transparent result is obtained if Bremsstrahlung is neglected. In this case, the relation

$$n T_i \hat{\tau}_E \geq \frac{6 T_i^2}{E_\alpha < \sigma v >} \frac{\tau_{E\alpha} + \tau_\alpha}{\tau_{E\alpha}} \left[1 + \sqrt{1 + \frac{1}{6} \frac{n < \sigma v > E_\alpha}{T_i} \frac{\tau_{E\alpha} \tau_{eq}}{k_1 k_2 (\tau_{E\alpha} + \tau_\alpha)}} \right]. \tag{12}$$

is obtained. One should notice that the right-hand side of Eq. (12), contrary to the original Lawson criterion, is not a function only of temperature, but also depends on plasma density through τ_{eq} and τ_α [see Eqs. (6) and (7)], even though the dependence on temperature is much stronger. A fixed value of $n = 10^{20}$ m^{-3} is used in the remainder of Section II. Incidentally, Eq. (12) depends on T_i and not T_e because the electron temperature was eliminated through (the time-independent version of) Eq. (2).

Both Eqs. (11) and (12) can be solved numerically once set to equalities. We do this by assigning T_i and n and calculating $\hat{\tau}_E$ with a Mathematica script freely available on [13]. Direct calculation shows that Bremsstrahlung only marginally affects the result. Since the inclusion of Bremsstrahlung does not complicate the numerical solution, all results shown in the following will include Bremsstrahlung. For clarity and for a meaningful comparison with the single-fluid case, here and in the rest of this work it is preferable to express the Lawson criterion using the plasma total pressure,

$$p_{tot} = p_i + p_e = n(T_i + T_e), \tag{13}$$

where in the single-fluid case $T_i = T_e = T$.

The results of the calculation are summarized in Fig. 1. The figure shows the value of $\tau_{Ei} = \hat{\tau}_E$ (on the left) and of the Lawson product (in the

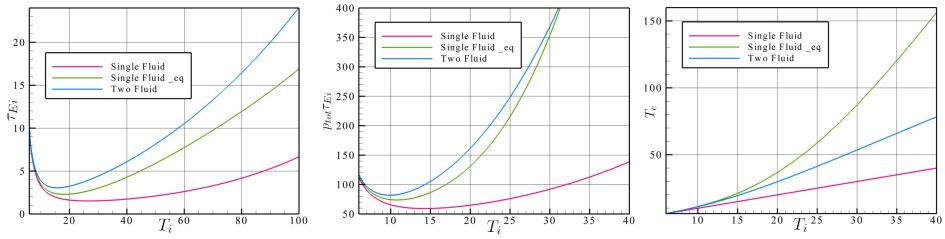

Figure 1: τ_{Ei} [s] vs. T_i (left), $p_{tot}\tau_{Ei}$ $\left[10^{20}\mathrm{m}^{-3}\mathrm{keV\ s}\right]$ vs. T_i (center) and T_e vs. T_i (right) for ignition for the single-fluid, "single-fluid equilibration" and two-fluid models. In this case all τ_E values are identical for the two-fluid model. Since $p_{tot}\tau_{Ei}$ and T_e grow rapidly for higher temperatures, the center and right plots cover a smaller T range.

center) needed for ignition, plotted versus the ion temperature T_i in keV. Three curves are included: the single-fluid (red), two-fluid (blue) and a curve dubbed "single-fluid$_{\mathrm{eq}}$" (green). The last curve is obtained using the complete two-fluid model, but setting $\tau_{Ee} = \tau_{Ei}$, $\tau_{E\alpha} \to \infty$ and $\tau_\alpha = 0$, meaning that the only difference between this model and the standard single-fluid model is the finite equilibration time between the ion and electron temperatures, which is set to the physical value given by Eq. (6). The two-fluid case considered in the calculation uses $\tau_{Ei} = \tau_{Ee} = \tau_{E\alpha} = \hat{\tau}_E$ and physical values for τ_{ei} and τ_α (equilibration time and α slowing-down time). It is seen that for any given temperature the two-fluid values are larger than the single-fluid ones. The energy confinement time (Fig. 1 left) needed for ignition in the single-fluid$_{\mathrm{eq}}$ model are intermediate between the complete single-fluid and two-fluid models. For increasing temperatures the two-fluid values grow much faster than the single-fluid ones, so much so that the $p_{tot}\tau_E$ plot (center) only extend to 40keV. Perhaps surprisingly, the single-fluid$_{\mathrm{eq}}$ curve crosses the two-fluid curve for sufficiently high values of the temperature. This is explained by the curves in Fig. 1 right, showing the electron temperature as a function of T_i for the three models. For any ion temperature, the largest electron temperature at ignition is found for the single-fluid$_{\mathrm{eq}}$ model. That is due to the fact that in this model all α power is immediately deposited into the electrons, but transferred to the ions at a finite rate. Since τ_{eq} is a strongly increasing function of temperature, larger temperature differences are found at higher ion temperatures. This result can be confirmed using the steady-state form of Eqs. (2-4). Coming back to

the center pane of Fig. 1, single- and two-fluid curves are qualitatively similar, but minima occur at lower temperatures in the two-fluid case ($T_i \sim$10 keV and $T_e \sim$11 keV vs. $T \sim$14 keV for the Lawson product).

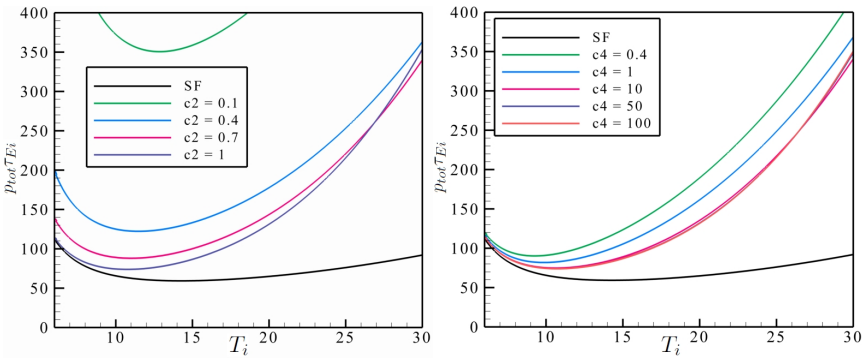

Figure 2: $p_{tot}\tau_{Ei}$ vs. T_i for ignition in 0D. Left: $c_2 \equiv \tau_{Ee}/\tau_{Ei}$ is varied, αs are perfectly confined. Right: $\tau_{Ee} = \tau_{Ei}$, $c_4 \equiv \tau_{E\alpha}/\tau_{Ei}$ is varied.

The next question to consider is the importance of the different energy confinement times in determining the minimum Lawson product needed for ignition. In particular, it is of interest to evaluate the effect of poor confinement for electrons and α particles. This is done in Fig. 2, which shows the minimum Lawson product (calculated with τ_{Ei}) as a function of T_i when the ratio τ_{Ee}/τ_{Ei} is varied (left) and when the ratio $\tau_{E\alpha}/\tau_{Ei}$ is varied (right). The physical value for τ_{eq} is used in all cases in Fig. 2. In the left plot (varying τ_{Ee}) $\tau_{E\alpha} \to \infty$, while in the right plot (varying $\tau_{E\alpha}$) $\tau_{Ee} = \tau_{Ei}$. It is seen that the Lawson product needed for ignition is fairly sensitive to the value of τ_{Ee}/τ_{Ei} even when αs are perfectly confined. On the other hand, the exact value of the ratio $\tau_{E\alpha}/\tau_{Ei}$ is less important. When the ratio is close to unity, changes only cause a slight shift of the curve and minimal changes in the minimum of the curve ($p_{tot}\tau_{Ei}|_{min} = 90.26$ $\left[10^{20}\mathrm{m}^{-3}\mathrm{keV\ s}\right]$ for a 0.4 ratio and 81.89 for a ratio of 1). Also, increasing $c_4 = \tau_{E\alpha}/\tau_{Ei}$ much above unity has a negligible effect, as the curves for $c_4 = 10$ and $c_4 = 100$ are almost identical. Note that the curves on the right pane of Fig. 2 will approach the single-fluid$_{\mathrm{eq}}$ curve for very large values of c_4. The apparently puzzling feature of the left figure, namely the fact that the curves for $\tau_{Ee}/\tau_{Ei} = 0.7$ and $\tau_{Ee}/\tau_{Ei} = 1$ cross for $T_i \simeq 27$keV is explained by the fact that with a lower electron energy confinement time the electron temperature will be lower for the same ion temperature. In these conditions ignition occurs for

a $\sim 10\%$ larger τ_{Ei} and thus a $\sim 10\%$ larger $nT_i\tau_{Ei}$. Furthermore, for sufficiently high temperatures the Lawson product $n(T_e + T_i)\tau_{Ei}$ turns out to be lower (because nT_e is lower) in the case with $\tau_{Ee}/\tau_{Ei} = 0.7$ than in the case with $\tau_{Ee}/\tau_{Ei} = 1$, even though the τ_{Ei} for ignition is larger.

More insight on the dependence of the Lawson product needed for ignition from the different energy confinement times can be gained looking back at Eq. (12) (as mentioned earlier, the effect of Bremsstrahlung can be neglected). In particular, it is seen that τ_α (slowing down time) and $\tau_{E\alpha}$ (alpha energy confinement time) always appear in the combination $\tau_\alpha/\tau_{E\alpha}$. For this reason, we write:

$$\frac{\tau_\alpha}{\tau_{E\alpha}} = \frac{\tau_\alpha}{\tau_{Ei}} \frac{\tau_{Ei}}{\tau_{Ee}} \frac{\tau_{Ee}}{\tau_{E\alpha}}. \tag{14}$$

Since τ_α has a physical expression:

$$\frac{\tau_\alpha}{\tau_{E\alpha}} = K \frac{T_e^{3/2}}{n\tau_{Ei}} \frac{(T_i + T_e)}{(T_i + T_e)} \frac{\tau_{Ei}}{\tau_{Ee}} \frac{\tau_{Ee}}{\tau_{E\alpha}} = K \frac{T_e^{3/2}(T_i + T_e)}{p\tau_{Ei}} \frac{\tau_{Ei}}{\tau_{Ee}} \frac{\tau_{Ee}}{\tau_{E\alpha}}, \tag{15}$$

where K is a dimensional constant. Thus we identify τ_{Ee}/τ_{Ei} and $\tau_{Ee}/\tau_{E\alpha}$ as meaningful parameters to vary. In an equivalent way, we chose to vary the parameters τ_{Ee}/τ_{Ei} and $\tau_{E\alpha}/\tau_{Ei}$, relating all energy confinement times to the ion energy confinement time. A large number of cases was run with $0.1 \leq \tau_{Ee}/\tau_{Ei} \leq 1$ and $0.1 \leq \tau_{E\alpha}/\tau_{Ei} \leq 10$. For each case, the minimum of $p_{tot}\tau_{Ei}$ needed for ignition was calculated. The results of the calculation are shown in Fig. 3. For the results in Fig. 3 the value of $p_{tot}\tau_{Ei}$ is well approximated by the expression:

$$p_{tot}\tau_{Ei} \simeq a_0 \left(1 + \frac{a_1}{c_2}\right) \left(1 + \frac{a_2}{c_4}\right) + \frac{a_3}{c_2 c_4} + a_4 \log(c_4), \tag{16}$$

with all a_j coefficients being listed in Table 1. Equation (16) allows to estimate the Lawson product needed for ignition for arbitrary values of the input parameters $c_2 \equiv \tau_{Ee}/\tau_{Ei}$ and $c_4 \equiv \tau_{E\alpha}/\tau_{Ei}$.

In addition to the Lawson product required for ignition the standard 0D, single-fluid treatment of the ignition problem also allows to calculate the minimum heating power needed to reach ignition starting from a cold plasma. This is done by calculating the time derivative of T from Eq. (5) assuming no heating power S_h. When calculated at different temperatures and plotted vs. T, this curve, the so-called $\dot{T}$ vs. T curve, [1] presents a (negative) minimum. A heating power $\hat{S}_h$ can be added to the equation to make the minimum of $\dot{T} = 0$. The value $\hat{S}_h$ is the minimum heating power needed

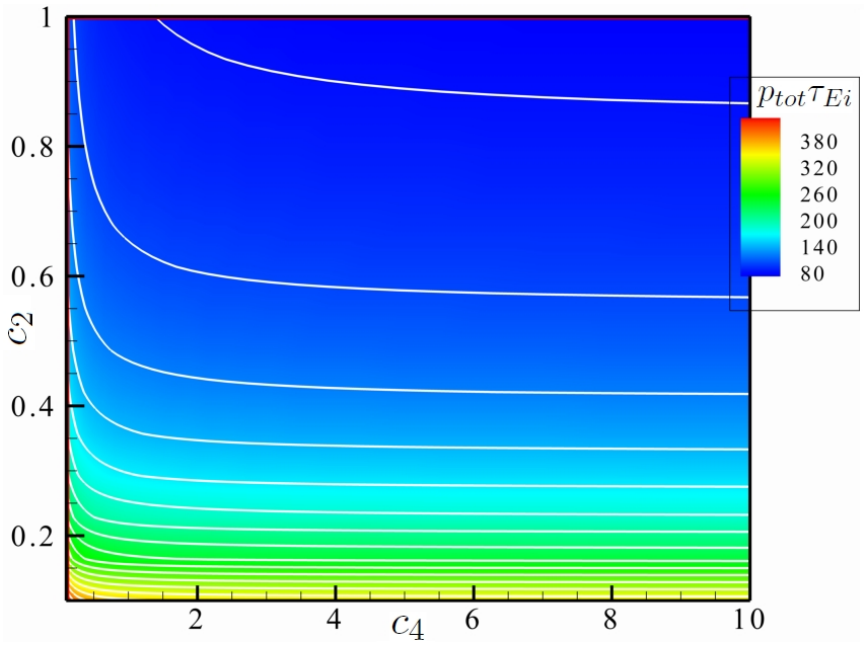

Figure 3: $p_{tot}\tau_{Ei}$ [$10^{20}\mathrm{m}^{-3}$ keV s] for ignition in 0D varying both $c_2 \equiv \tau_{Ee}/\tau_{Ei}$ and $c_4 \equiv \tau_{E\alpha}/\tau_{Ei}$. For each couple of values (c_2, c_4) the minimum $p_{tot}\tau_{Ei}$ for ignition is shown.

Coefficient	Value
a_0	50.0744
a_1	0.616194
a_2	0.0558493
a_3	-1.18581
a_4	-2.92248

Table 1: Approximate fit for $p_{tot}\tau_{Ei}$ varying $c_2 \equiv \tau_{Ee}/\tau_{Ei}$ and $c_4 \equiv \tau_{E\alpha}/\tau_{Ei}$ (0D case). The maximum relative error of $\sim 4.5\%$ occurs at the lower-right corner of Fig. 3. The average error is $\sim 0.9\%$.

for the bootstrapping of the plasma temperature to achieve the ignition conditions. Heating power can be turned off once the plasma temperature has reached the ignition temperature. Curves for $\dot{T}$ vs. T for different models are shown later in Fig. 11. The model developed for multi-fluid ignition calculation allows to estimate the effects of the various parameters present in the system on the minimum heating power needed to achieve ignition. In this analysis it is assumed for simplicity that, contrary to more detailed calculations [14,15], energy confinement times do not depend on the heating power. Therefore, issues such as identifying the optimal heating path to ignition (the "Cordey pass" [16]) are not considered in this work. Numerical results for this calculation are presented next.

First, the effect of the α slowing down time τ_α is considered. The reasoning is that if α particles take a long time to transfer their energy to the electrons, a large fraction of the energy produced by fusion reaction will be lost before it reaches the ions. Numerical results are shown in Fig. 4. The figure shows $S_h\tau_{Ei}$, the minimum heating power needed for ignition multiplied by the ion energy confinement time, vs. τ_{Ei} (left) and vs. the ignition temperature (right) for different values of the slowing down time τ_α. The heating power is shown in arbitrary units, but the same units are used in all calculations in Section II. In order to isolate the effect of τ_α, this calculation is done in the single-fluid limit, setting $\tau_{Ee} = \tau_{Ei}$, $\tau_{eq} = 0$ and $\tau_{E\alpha} \to \infty$, while τ_α is assumed to be proportional to τ_{Ei}, with the proportionality constant being varied between 0.1 and 10. Looking at Eq. (12), it is seen that with these choices the Lawson product does *not* depend on τ_α. Figure 4 shows that the heating power needed for ignition is fairly insensitive to the value of τ_α, only showing some small change when τ_α becomes much larger than τ_{Ei}. Note that the physical value of τ_α is smaller than the considered

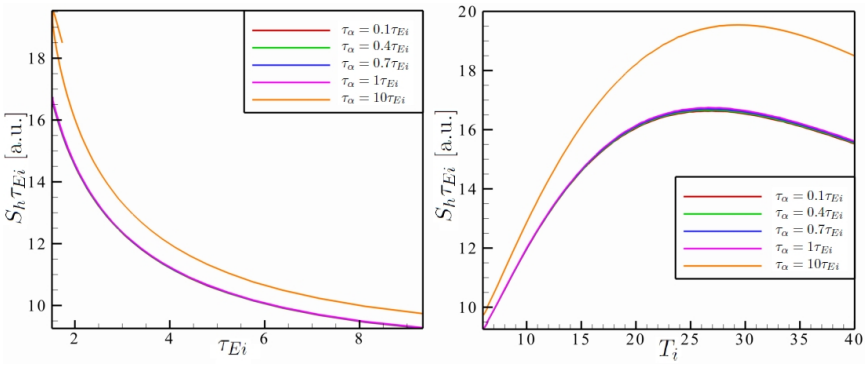

Figure 4: Effect on heating power to reach ignition of varying τ_α with $\tau_{Ei} = \tau_{Ee}$, $\tau_{eq} = 0$ and $\tau_{E\alpha} \to \infty$., plotted vs. τ_{Ei} [s] (left) and T_i [keV] (right). (τ_α = slowing-down time)

τ_{Ei}. The $\tau_\alpha = 10\tau_{Ei}$ curve is double-valued for small values of τ_{Ei}. That is explained as follows. All curves were obtained numerically for a range of ignition temperatures that goes beyond the minimum in τ_{Ei} for ignition (see Fig. 1 for the curve τ_E vs. T). This means that for a range of values of τ_{Ei} two ignition values of T_i are found for the same value of τ_{Ei}. In the single-fluid case the plasma will spontaneously transition to the higher ignition temperature if the lower one is reached, so that the same heating power is sufficient to reach both ignition temperatures. Something similar happens in the two-fluid model, except for the case where the slowing down time is long with respect to the energy confinement time. In that case, not enough of the α power may be transferred to the ions to increase the temperature to the higher ignition point. The result is that additional heating is needed to reach the higher ignition point, even though the two ignition temperatures require the same energy confinement time.

Some more information on the effect of τ_α on the heating power needed for ignition is presented in Fig. 5. The figure shows two curves (plotted both versus τ_{Ei} and T_i) for different values of τ_α, the physical one and $\tau_\alpha = 0$. In this case, the physical value was used for τ_{eq} and $\tau_{Ee}/\tau_{Ei} = 1$. The two curves are almost indistinguishable. This is due to the fact that in Fig. 5 the important parameter for determining the minimum heating power needed to reach ignition temperature is the α slowing down time at the minimum of $\dot{T}$. Direct calculation shows that for the parameters in Fig. 5 $(\tau_{\alpha;phys}/\tau_{Ei}) \sim 1\% - 5\%$, i.e. that τ_α is negligibly small. A similar

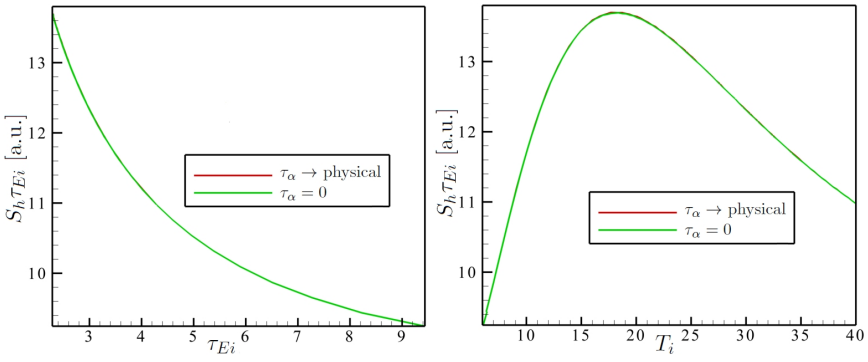

Figure 5: Heating power needed to reach ignition using the physical value for τ_{eq}, $\tau_{Ee}/\tau_{Ei} = 1$ and considering the physical value for τ_α and $\tau_\alpha = 0$. (τ_α = slowing-down time)

result (not shown) is obtained if a different τ_{Ee}/τ_{Ei} ratio is assumed. The conclusion is that the inclusion of the physical slowing down time in heating power for ignition calculations does not affect the result. However, if the slowing down time was much longer than the energy confinement time a larger heating power would be required to reach ignition.

Next, we consider the effect of τ_{Ee} alone. This is done by considering different ratios τ_{Ee}/τ_{Ei}, keeping $\tau_{E\alpha} \to \infty$ and physical values for τ_{eq} and τ_α. A small value of τ_{Ee}/τ_{Ei} requires an unrealistically large value of τ_{Ei} ($\tau_{Ei} > 10$s) to reach ignition and a large heating power. For this reason the red curve ($\tau_{Ee}/\tau_{Ei} = 0.1$) is out of the range of τ_{Ei} values shown in Fig. 6. Even a relatively small change in the ratio produces measurable changes in the heating power and the ion energy confinement time needed for ignition. We conclude that the electron energy confinement time is an important parameter not only for determining the minimum Lawson product for ignition but also for the amount of heating power needed to reach ignition.

The last parameter of interest is the α particle energy confinement time, the effect of which is evaluated by changing the parameter $\tau_{E\alpha}/\tau_{Ei}$ from 0.1 to 10, keeping $\tau_{Ee}/\tau_{Ei} = 1$ and physical values for τ_{eq} and τ_α. The results of the calculation are shown in Fig. 7. It is seen that the amount of heating power needed for ignition is fairly insensitive to $\tau_{E\alpha}$, at least as long as the α sowing down time is much shorter than $\tau_{E\alpha}$. A small value of $\tau_{E\alpha}$ requires a larger amount of heating at the same ion energy confinement time, but less heating at the same ion ignition temperature. This is explained observing

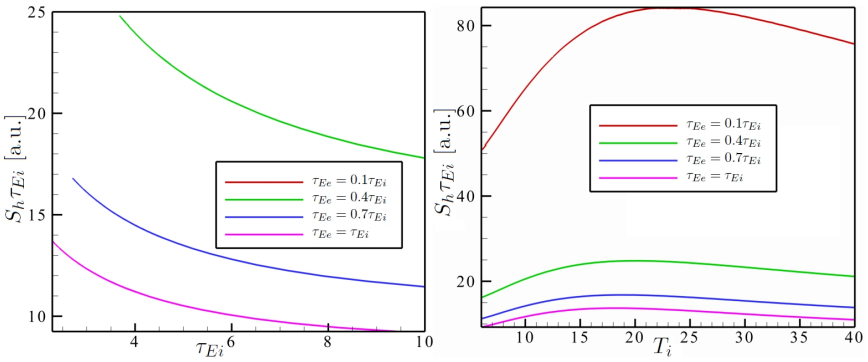

Figure 6: Effect of τ_{Ee}/τ_{Ei} alone on the heating power needed to reach ignition, keeping $\tau_{E\alpha} \to \infty$, τ_{eq} and τ_α physical.

that a given ignition temperature is reached with smaller τ_{Ei} if $\tau_{E\alpha}$ is larger implying that the minimum value of $\dot{T}$ is lower. Also, the horizontal axes in the two plots are not simply proportional to each other. Finally, it is worthwhile to emphasize that the effect of a change in $\tau_{E\alpha}$ is much smaller that the effect of changing τ_{Ee}.

III One-Dimensional Analysis of Ignition

In the present section we describe how to improve the well-known Lawson criterion moving from the original 0D approximation to assuming one-dimensional profiles for all physical quantities in Eqs. (2-4). All the multi-fluid physical effects described in the previous Section II are still taken into account in the one-dimensional case.

One-dimensional effects are analyzed using a parametric approach. Density and temperature profiles are parametrized as:

$$n(r,t) \equiv n_0(t)\hat{n}(r;\eta,\theta), \tag{17}$$

$$T(r,t) \equiv T_0(t)\hat{T}(r;\mu,\nu), \tag{18}$$

with

$$\hat{n}(r;\eta,\theta) = \hat{n}_{edge} + (1-\hat{n}_{edge})\left(1-r^\theta\right)^\eta, \tag{19}$$

$$\hat{T}(r;\mu,\nu) = \hat{T}_{edge} + (1-\hat{T}_{edge})\left(1-r^\nu\right)^\mu, \tag{20}$$

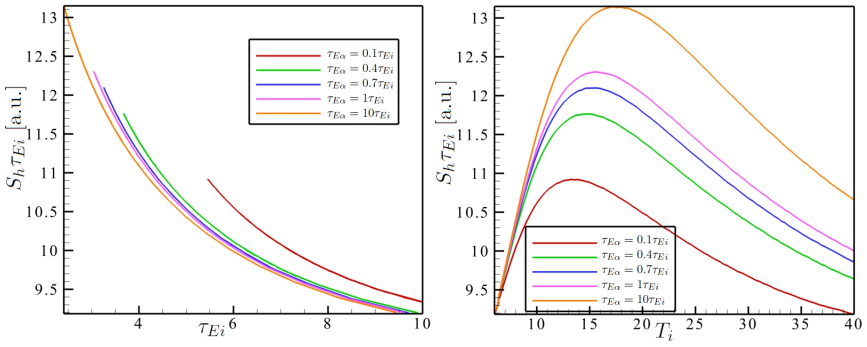

Figure 7: Effect on heating power for ignition of changing $\tau_{E\alpha}$ from $0.1\tau_{Ei}$ to $10\tau_{Ei}$, keeping $\tau_{Ee}/\tau_{Ei} = 1$ and physical values for τ_{eq} and τ_{α}

where r is a radial variable normalized to unity at the plasma edge, "hatted" profiles are dimensionless and normalized to unity in the plasma center ($r = 0$) and $\hat{n}_{edge}$ and $\hat{T}_{edge}$ are some arbitrarily small edge values for the profile function ($10^{-3} - 10^{-5}$ in the rest of this work). Due to quasi-neutrality, the density profile is assumed to be identical for ions and electrons. Ion and electron temperature profiles could in principle be different (and this is implemented in the Mathematica notebooks we used for our work, see [13]), but are assumed to be identical in the remainder of this work for simplicity. Note however that the central values $T_0(t)$ for ions and electrons are different and evolving separately. The profiles corresponding to the limiting values of the parameters are shown in Fig. 8 (left). In preliminary work, the same limiting values were used for both density and temperature in the investigation of the effect of one-dimensional profiles. However, one should keep in mind that in experiments a certain amount of control on the density profile is going to be available e.g. through fueling, while the temperature profile is determined by transport and thus less easily controlled. For this reason, only two temperature profiles, approximating typical L- and H-mode tokamak temperature profiles, were used in this work. The temperature reference profiles are shown in Fig. 8 (right). They will be referred to as "L-mode" and "H-mode" temperature profiles for the remainder of this work. Different profiles can easily be introduced in the Mathematica solver if desired. Once more, Mathematica notebooks are freely available on [13].

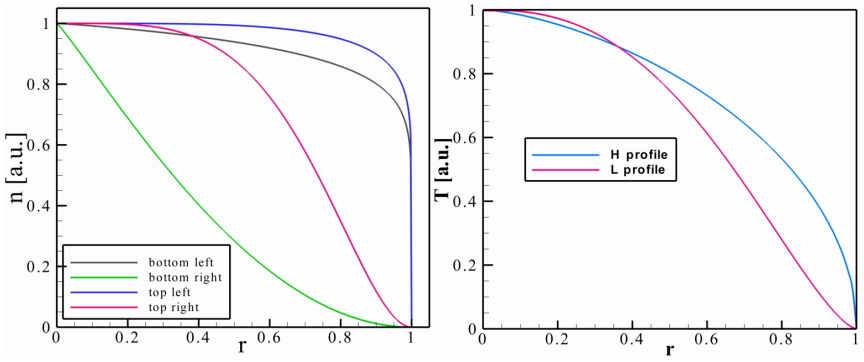

Figure 8: Left: Limiting profiles for parametric scan. Labels refer to figures in Section III. Note that all profiles have 0 derivative on axis. Right: L- ($\mu = 1.5$, $\nu = 2.5$) and H-mode ($\mu = 0.5$, $\nu = 1.5$) reference temperature profiles used in this work.

Lastly, a profile for the α particle density is also needed. This is determined at each time step solving for the equilibrium profile $n_\alpha(r,t)$ in

$$\cancelto{0}{\frac{\partial n_\alpha(r,t)}{\partial t}} = \frac{n(r,t)^2}{4} < \sigma v > (r,t) - \frac{n_\alpha(r,t)}{\tau_\alpha(r,t)} - \frac{n_\alpha(r,t)}{\tau_{E\alpha}}. \tag{21}$$

In other words, the spatial profile is obtained balancing sources and losses of αs. This balance is satisfied exactly only at steady state. However, solving for the shape of n_α in Eq. (21) gives a plausible profile for the α particle density. The profile obtained form Eq. (21) is normalized to unity at $r = 0$, so that

$$n_\alpha(r,t) \equiv n_{\alpha,0}(t)\hat{n}_\alpha(r), \tag{22}$$

where $\hat{n}_\alpha(r)$ is the normalized solution of Eq. (21) and is calculated at each time step. However, in each time step the profile $\hat{n}_\alpha$ is kept fixed when taking time derivatives and time-dependent equations are solved for $n_{\alpha,0}(t)$. Arguably, this is the most strongly simplifying assumption in the analysis. As shown in Ref. [11], in a tokamak configuration the thermonuclear instability corresponding to ignition is expected to develop with a 'quasi-flute' three-dimensional structure starting from rational surfaces. In order to include this result in the model presented here, one should replace the profile given by Eq. (21) with a three-dimensional profile built on the eigenfunction shape given in Ref. [11].

The time-dependent behavior of the system is described by the following Eqs. (23-25):

$$\frac{3}{2}n(r,t)\frac{\partial T_i(r,t)}{\partial t} = S_{hi} - \frac{3}{2}\frac{n(r,t)T_i(r,t)}{\tau_{Ei}} + \frac{3}{2}\frac{n(r,t)\left(T_e(r,t) - T_i(r,t)\right)}{\tau_{eq}}, \tag{23}$$

$$\begin{aligned}\frac{3}{2}n(r,t)\frac{\partial T_e(r,t)}{\partial t} &= S_{he} - \frac{3}{2}\frac{n(r,t)T_e(r,t)}{\tau_{Ee}} + \frac{n_\alpha(r,t)}{\tau_\alpha}E_\alpha \\ &\quad - C_B\frac{\left(n(r,t)T_e^2(r,t)\right)}{T_e^{3/2}(r,t)} + \frac{3}{2}\frac{n(r,t)\left(T_i(r,t) - T_e(r,t)\right)}{\tau_{eq}},\end{aligned} \tag{24}$$

$$\frac{\partial n_\alpha(r,t)}{\partial t} = \frac{n^2(r,t)}{4} < \sigma v > - \frac{n_\alpha(r,t)}{\tau_\alpha} - \frac{n_\alpha(r,t)}{\tau_{E\alpha}}. \tag{25}$$

One should keep in mind that $< \sigma v >=< \sigma v > (T_i(r,t))$, $\tau_\alpha = \tau_\alpha\left(n(r,t), T_e(r,t)\right)$ and $\tau_{eq} = \tau_{eq}\left(n(r,t), T_i(r,t), T_e(r,t)\right)$, while the energy confinement times $\tau_{Ei}, \tau_{Ee}, \tau_{E\alpha}$ are entered as constant values for each case. For time-dependent calculations, Eqs. (23-25) are integrated over the plasma volume at each time step, then advanced in time as a system of ODEs. If the α-particle three-dimensional profile of Ref. [11] was considered, the energy balance equations should also include three-dimensional modifications to the temperature profiles. Integrations over the plasma volume would then have the additional computational cost caused by the three-dimensional geometry of the profiles. However, since the actual energy balance and time evolutions are evaluated after the volume integration, one may expect that the modifications to the results of this paper due to more detailed three-dimensional profiles will be more of a quantitative than qualitative nature. All calculations where performed with the software package Mathematica.

A variety of density profiles [i.e., values of η and θ in Eq. (19)] are considered for each temperature profile (L-mode and H-mode). For reference, an "L-mode-like" density profile is approximated by $\eta = 1.25$, $\theta = 2.25$ and an "H-mode-like" density profile is approximated by $\eta = 0.25$, $\theta = 1.25$. For each combination of temperature and density profiles, the minimum Lawson product $p_{tot}\tau_{Ei}$ needed for ignition is calculated numerically. The results of the calculations are shown in Fig. 9. For the results in Fig. 9, $\tau_{Ee} = \tau_{E\alpha} = \tau_{Ei}$ and physical values are used for equilibration times. As the density profile is changed in Fig. 9, the peak value is adjusted so that all calculations are done with the same average density. However, it was verified with direct numerical calculation that essentially identical results

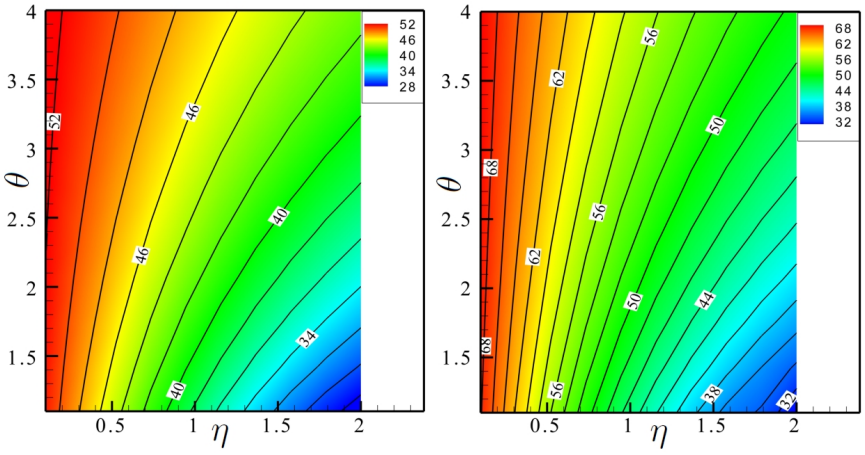

Figure 9: Minimum $p_{tot}\tau_{Ei}$ for ignition in $10^{20}\mathrm{m}^{-3}$ keV s as function of density profile for the L- (left) and H- (right) mode temperature profiles. Color scales are different in the two plots. For reference, the 0D value is $\simeq 82$ [$10^{20}\mathrm{m}^{-3}$ keV s].

for $p_{tot}\tau_{Ei}$ are obtained if the central density value is kept constant instead, confirming that the Lawson product depends weakly on the magnitude of the density also in the one-dimensional case, as was observed earlier for the 0D case [see Eq. (12)]. It can be seen that one-dimensional profiles decrease the minimum Lawson product necessary for ignition with respect to the 0D value. Moreover, peaked profiles (lower right corner of the figures) require lower Lawson products than flat profiles. This is further confirmed by observing that for the same density profile, a peaked temperature profile (as in L-mode profile, left part of the Fig. 9) requires a lower Lawson product than a flatter temperature profile (as in H-mode profile, right part of the figure). This is in qualitative agreement with the results of Ref. [17]. However, keeping the density profile the same, an H-mode temperature profile requires a Lawson product 10-30% larger than an L-mode temperature profile, while the energy confinement time in H-mode is typically $\gtrsim 2$ times [18] larger than the energy confinement time achieved in L-mode. The exact ratio between Lawson products in the L- and H-mode of operation for a given experimental design will also depend on the density profile of each mode of operation. Not shown in Fig. 9 but worth mentioning is the fact that with one-dimensional profiles the minimum of the Lawson product needed for ig-

nition is reached with ion *peak* temperatures of 10-14 keV and thus *average* ion temperatures ≃4.6–8.5keV, considerably smaller than what predicted by the Lawson 0D, single-fluid model (≃ 14.3keV).

The triple product needed for ignition in the one-dimensional case can be expressed with approximated formulas. The best fit is found with the formula:

$$\frac{p_{tot}\tau_{Ei}}{(p_{tot}\tau_{Ei})_{0D}} \simeq f_0 \left(\left(1 + f_1\eta + f_2\eta^2\right) \left(1 + f_3\theta + f_4\theta^2\right) + f_5\eta\theta + f_6\eta^2\theta + f_7\eta\theta^2 + f_8\eta^2\theta^2 \right), \tag{26}$$

which gives an average relative error of $\sim 0.36\%$ in the L-mode case and $\sim 0.48\%$ in the H-mode case, with maximum errors $\simeq 1\%$ in both cases. The f_j coefficients for the formula are given in Table 2. A simpler formula,

Coefficient	L-mode	H-mode
f_0	0.649512	0.871336
f_1	-0.483244	-0.594539
f_2	0.0692349	0.111705
f_3	-0.000559668	-0.00377657
f_4	0.00024973	0.000664823
f_5	0.15341	0.154859
f_6	-0.0255369	-0.0330017
f_7	-0.0158339	-0.015922
f_8	0.00270186	0.00367627

Table 2: Coefficients for the interpolation formula given by Eq. (26)

which gives an average error of $\simeq 3.7\%$ (L-mode) and $\simeq 3.9\%$ (H-mode) and maximum errors of $\simeq 10\%$ and $\simeq 12\%$ is written as

$$\frac{p_{tot}\tau_{Ei}}{(p_{tot}\tau_{Ei})_{0D}} \simeq g_0 \left(\left(1 + g_1\eta\right) \left(1 + g_2\theta\right) + g_3\eta^2\theta^2 \right). \tag{27}$$

Coefficients are given in Table 3.

Qualitatively similar results are obtained if different assumptions are made on the various characteristic times in Eqs. (2-4). Results for two more cases are shown in Fig. 10 and compared to the "standard" case (with $\tau_{Ei} = \tau_{Ee} = \tau_{E\alpha}$) and the single-fluid case. The additional cases included in Fig. 10 have $c_2 \equiv \tau_{Ee}/\tau_{Ei} = 0.1$, $\tau_{E\alpha} = \tau_{Ei}$ (blue curve) and $c_4 \equiv \tau_{E\alpha}/\tau_{Ei} = 0.1$, $\tau_{Ee} = \tau_{Ei}$ (red curve). Physical equilibration and α slowing down times are used in all calculations. For the plots in Fig. 10 the density profile is defined

Coefficient	L-mode	H-mode
g_0	0.59373	0.78304
g_1	-0.22066	-0.273862
g_2	0.0388736	0.0351134
g_3	0.0045117	0.00488574

Table 3: Coefficients for the interpolation formula given by Eq. (27)

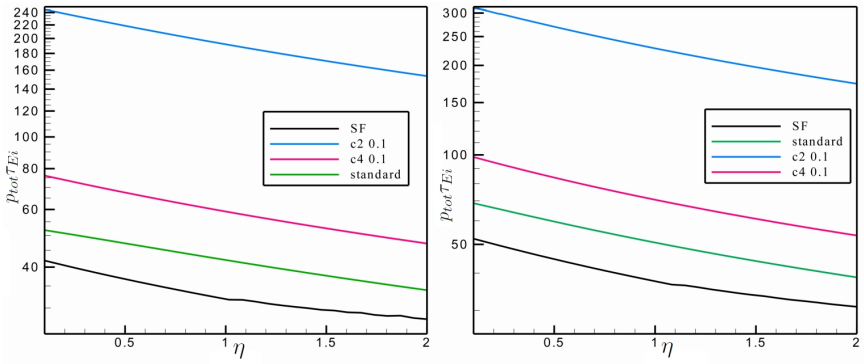

Figure 10: Effect of density peaking factor on $p_{tot}\tau_{Ei}$ (in log scale and in $10^{20}\mathrm{m}^{-3}$ keV s) for L- (left) and H-mode (right) temperature profiles. Peaking factor is given by $\eta + 1$, so that peaked profiles are on the right ($\eta \simeq 2$), flat profiles left ($\eta \simeq 0$). Vertical scales on the two plots are different.

as

$$\hat{n}(r;\eta) = \hat{n}_{edge} + (1 - \hat{n}_{edge})\left(1 - r^2\right)^{\eta}, \tag{28}$$

i.e. $\theta = 2$ for all profiles. With this definition, the density peaking factor is given by $\hat{n}(0;\eta)/ < \hat{n}(r;\eta) >= \eta + 1$. The curves in Fig. 10 represent the Lawson product calculated using τ_{Ei} as a function of density peaking for the L- (left) and H-mode (right) temperature profiles. It is seen that the most critical parameter is the electron energy confinement time, while the effect of the α particle energy confinement time is much weaker. Notably, the ratio between the Lawson product at $\eta = 0.1$ and $\eta = 2$ is approximately 1.6 for all the L-mode curves and $\sim$1.8 for all H-mode curves.

To conclude this section, we consider the effect of the additional physics introduced in this work on the traditional $\dot{T}$ vs. T curve. The curves in Fig. 11 show the time derivative of T_i in [keV/s] as a function of the peak value

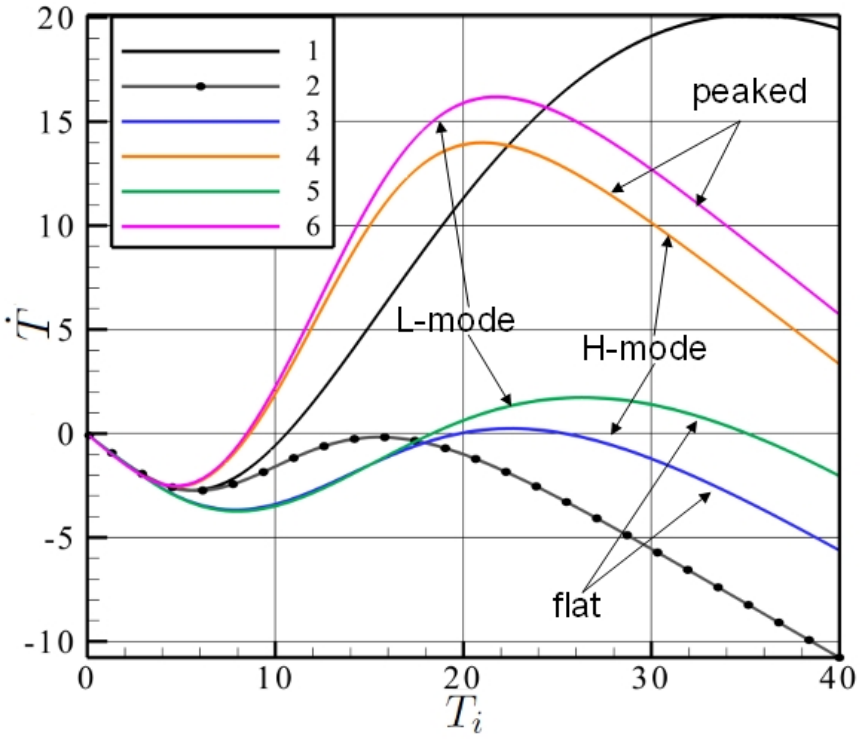

Figure 11: $\dot{T}$ vs. T_i for: the single-fluid 0D model (1); the two-fluid 0D model (2); the H-mode temperature profile with $\theta = 2$ and $\eta = 0.1$ (3), $\eta = 2$ (4); the L-mode temperature profile with $\theta = 2$ and $\eta = 0.1$ (5), $\eta = 2$ (6). For the 1D profiles, T_i is the peak temperature.

of T_i. This is calculated by fixing T_i and solving to steady state Eqs. (3-4), then substitute the steady-state values of T_e and n_α to calculate the left-hand side of Eq. (2). Figure 11 includes a curve for the 0D single-fluid (curve 1) and two-fluid (curve 2) case for comparison with the 1D curves. Both the H- and L-mode temperature profiles are used. For each temperature profile, two values of η with a fixed value of $\theta = 2$ are used, corresponding to peaking factors of 1.1 ($\eta = 0.1$) and 3 ($\eta = 2$). A value of $\tau_E = 3$s is used for all energy confinement times and all cases. Also, all cases have the same average density of 10^{20} m^{-3}. All $\dot{T}$ curves start from 0 at $T = 0$ and keep decreasing until a minimum is passed. Depending on the case, a positive $\dot{T}$ value may or may not be reached. The point of zero crossing corresponds to ignition. It is seen that the 0D two-fluid case does not reach ignition,

while all 1D cases do. For flat density profiles ($\eta = 0.1$, curve 3 for H-mode temperature profile and curve 5 for L-mode temperature profile) ignition is reached for higher temperatures than for peaked density profiles ($\eta = 2$, curve 4 for H-mode temperature profile and curve 6 for L-mode temperature profile). Also, the two zero crossings are much closer to each other in the flat density than in the peaked density case, corresponding to a condition closer to marginal ignition, where "marginal ignition" is the case of a curve tangent to the horizontal axis at the ignition point. Finally, a more peaked temperature profile (L-mode case) gives a higher performance (lower ignition point, higher $\dot{T}$) than a flat temperature profile (H-mode case).

IV Conclusions

In this work, the well known Lawson ignition criterion [5] was revisited and extended to include the effect of multi-fluid physics and one-dimensional density and temperature profiles.

Starting with a multi-fluid 0D model, different energy confinement times (a separate one for each species, ions, electrons and α particles) and energy equilibration times (between α particles and electrons and between ions and electrons) were introduced. Lawson's results are recovered assuming vanishing equilibration times and infinite α energy confinement time. A new ignition criterion, Eq. (12), was written and used to show the detrimental effect of the inclusion of multi-fluid physics, which increases the minimum Lawson product needed for ignition. Expressions for equilibration times are known from transport [1, 19], while uncertainty remains in energy confinement times, which are treated as free parameters in the calculations in this work. It was found that the electron energy confinement time is the most critical parameter in determining the Lawson product needed for ignition, while the Lawson product is less sensitive to the α energy confinement time, in the sense that small variations of the ratio τ_{Ee}/τ_{Ei} have a stronger effect on the Lawson product needed for ignition than similar variations of the ratio $\tau_{E\alpha}/\tau_{Ei}$ (see e.g. Fig. 10). It is stressed that an α energy confinement time much smaller than the ion energy confinement time, due for instance to toroidal Alfvén eigenmodes or fishbones [20], will make the Lawson product for ignition extremely large [see for instance Eq. (12)]. Therefore, α confinement is a crucial topic in ignition studies. An approximated formula, Eq. (16), was obtained to calculate the effect of varying electron and α energy confinement times on the ignition Lawson product.

The multi-fluid 0D model was also used to evaluate the heating power needed to reach ignition starting from a cold plasma. Heating was assumed to be only applied to the ions. The heating power for ignition also depends on the various parameters considered in this work. Once again, it is found that the most critical parameter is the electron energy confinement time, as poorly confined electrons require a larger heating power to reach ignition (even though no heating is directly applied to the electrons).

The one-dimensional model introduced in this work allows for different radial profiles of the density (assuming quasi-neutrality and neglecting the contribution of αs to charge balance ions and electrons have the same density profile) and ion and electron temperatures. The same shape (but with different maximum values) was used for the two temperatures, but the implementation allows in principle for arbitrary and different temperature profiles for ions and electrons. Density and temperature profiles are controlled independently in a parametric way [Eqs. (19) and (20)]. The combination of different density and temperature profiles gives a wide parametric space to be explored. Since temperature profiles are determined by transport and much harder to control in experiments than the density profile, only two temperature profiles, approximating typical L- and H-mode profiles, were considered in this work. Varying the density profiles it was found that both density and temperature peaked profiles require a lower Lawson product for ignition than flatter profiles, i.e., for a given temperature profile a flatter density profile will require a larger Lawson product and for a given density profile a flatter temperature profile will require a larger Lawson product. This is a very encouraging result for future experiments, since the widely used 0D Lawson result may overestimate the Lawson product needed for ignition. In the one-dimensional case, Lawson products are calculated integrating $n(T_e + T_i)$ over the plasma volume.

The effect of different α and electron energy confinement times on the ignition Lawson product was also investigated. Analogously to the 0D result, it was found that the electron energy confinement time is the parameter with the stronger effect on ignition.

Using the traditional $\dot{T}$ vs. T plot it was also shown that lower $\dot{T}$ (i.e., larger heating power required for ignition) is obtained for the two-fluid case as compared with the single-fluid one. Peaked profiles produce larger values of $\dot{T}$ than flat profiles and thus require a lower amount of heating to reach ignition. This applies to both density and temperature profiles.

V Acknowledgments

This work was performed under DOE grant DE-FG02-93ER54215.

References

[1] J. P. Freidberg, *Plasma Physics and Fusion Energy*, Cambridge University Press, Cambridge UK, 2007.

[2] IAEA, *Summary of the ITER Final Design Report*, Number 22 in ITER EDA Documentation Series, International Atomic Energy Agency, Vienna, 2001.

[3] J. Wesson, *Tokamaks*, Clarendon Press, Oxford, UK, 3rd edition, 2004.

[4] United States, Department of Energy, Office of Science and United States, Department of Energy, Office of Scientific and Technical Information, *Review of Burning Plasma Physics. Fusion Energy Sciences Advisory Committee (FESAC).*, United States, Department of Energy, Office of Science, 2001.

[5] J. D. Lawson, Proc. Phys. Soc. London **Sect. B 70**, 6 (1957).

[6] J. Kesner and R. Conn, Nucl. Fusion **16**, 397 (1976).

[7] B. C. Maglich and R. A. Miller, J. Appl. Phys. **46**, 2915 (1975).

[8] J. R. Treglio, J. Appl. Phys. **46**, 4344 (1975).

[9] B. Khosrowpour and N. Nassiri-Mofakham, Journal of Fusion Energy **35**, 513 (2016).

[10] A. Cardinali and G. Sonnino, Eur. Phys. J. D **69**, 194 (2015).

[11] B. Coppi, A. Airoldi, R. Albanese, G. Ambrosino, G. Belforte, E. Boggio-Sella, A. Cardinali, G. Cenacchi, F. Conti, E. Costa, A. D'Amico, P. Detragiache, G. D. Tommasi, A. DeVellis, G. Faelli, P. Ferraris, A. Frattolillo, F. Giammanco, G. Grasso, M. Lazzaretti, S. Mantovani, L. Merriman, S. Migliori, R. Napoli, A. Perona, S. Pierattini, A. Pironti, G. Ramogida, G. Rubinacci, M. Sassi, A. Sestero, S. Spillantini, M. Tavani, A. Tumino, F. Villone, and L. Zucchi, Nucl. Fusion **55**, 053011 (2015).

[12] R. Betti and J. P. Freidberg, Phys. Plasmas **4**, 1465 (1992).

[13] `http://www.auburn.edu/cosam/faculty/physics/guazzotto/research/TF_Lawson_main.html`.

[14] H. Furth, R. Goldston, S. Zweben, and D. Sigmar, Nucl. Fusion **30**, 1799 (1990).

[15] R. J. Goldston, Plasma Phys. Control. Fusion **26**, 87 (1984).

[16] J. Cordey, in *Physics of Plasmas in Thermonuclear Regimes (Proc. Workshop Varenna, 1979)*, Washington, DC, 1981, USDOE CONF-790866, United States Department of Energy.

[17] B. Coppi, A. Airoldi, F. Bombarda, G. Cenacchi, P. Detragiache, and L. Sugiyama, Nucl. Fusion **41**, 1253 (2001).

[18] ITER Physics Expert Group on Confinement and Transport et al., Nucl. Fusion **39**, 2175 (1999).

[19] J. D. Huba, *NRL PLASMA FORMULARY Supported by The Office of Naval Research*, Naval Research Laboratory, Washington, DC, 2013.

[20] W. W. Heidbrink, Phys. Plasmas **15**, 055501 (2008).